Indian Journal of Chemical Technology
Vol. 26, May 2019, pp. 205-215

Performance of polymer coagulants for colour removal from dye simulated medium: Polymer adsorption studies

O D Onukwuli*,[1] & I A Obiora-Okafo[2]

[1]Department of Chemical Engineering, NnamdiAzikiwe University, Awka, Nigeria.

[2]Department of Chemical Engineering, Madonna University, Elele, Nigeria.

E-mail: onukwuliod@yahoo.com

Received 7 September 2016; accepted 29 November 2018

Evaluation of natural coagulants for colour removal from dye simulated wastewater has been studied. The proximate compositions and surface morphologies of the organic polymers are investigated. The effects of operational parameters including *p*H, coagulant dosage, dye concentration, settling time and temperature are tested and their optimum operating ranges determined. Acidic solution *p*H increased the colour removal efficiency. Accurate control of coagulant dosages is required for optimum destabilization of charged particles. Dye concentration is a driving force that shows the extent of particle transfer. Polymer performances on the flocculation process are measured through time-dependent decrease in particle concentrations and consequently, promoting flocs growth. Charge neutralization, polymer adsorption, inter-particle bridging and sweep-flocculation are the active mechanisms in the removal process. Adsorption of particles on the polymer surfaces occur mostly as a monomolecular layer and according to chemisorption mechanism. The agreement of pseudo-second order and Elovich model with high correlation (R^2>0.926) confirms the coagulation-flocculation/adsorption kinetics behaving more as a second-order rate process.

Keywords: Coagulation-flocculation**,** Azocarmine G, Colour removal, Polymer coagulants, Polymer adsorptions.

Coagulation-flocculation process in recent studies removes different contaminants from water and wastewater including both organic and inorganic contaminants[1, 2]. Colour is a major contaminantfound in most industrial wastewater, and has been effectively removed using coagulation-flocculation technique[2, 3]. Studies on improving the coagulation-flocculation process have attracted attentions and its performance is largely affected by the type of coagulant used. Achoice of coagulant enhances the aggregation of particles for large flocs formation capable of rapid settling through charge neutralization, enmeshment in a precipitate, double layer compression, inter-particle bridging and adsorption mechanisms. These mechanisms of particles flocculation are more experienced using natural polyelectrolytes of high molecular weight as coagulants.The use of natural coagulants (organic polymers) for water treatment has improved coagulation-flocculation process[4]. Natural coagulants are anionic, cationic or non-ionic in nature and are collectively termed polyelectrolyte due to their ionic nature. Comprehensive studies of water-soluble polyelectrolyte coagulants were given by Bolto and Gregory[5].

Natural coagulants are of emerging trend by many researchers because of their abundant source, low price, environmental friendly, multifunction, and biodegradable in water. Mechanisms of particles flocculation by natural polymers were described by charge neutralization, polymer adsorption, sweep-flocculation, inter-particle bridging, and electrostatic patch mechanisms. Polymer adsorption plays important roles in the activities of other mechanisms. Polymer adsorption occurs when there are attractions between polymer segments and particle surfaces. Adsorption interactions are possible by electrostatic interaction, hydrogen bonding and ion bonding[5]. Electrostatic interaction is most important which occurs due to presence of charged particles. Electrostatic interaction occurs when polyelectrolytes with a charge opposite to that of the surface (cationic polyelectrolytes on negative surfaces) absorb strongly, simply because of attraction between opposite charge ionic groups.

Polymeric coagulants when dosed into particles suspension, initiates several processes as shown in Fig. 1[5]. a) Polymer added to the concentrated solution is evenly distributed throughout the suspension. b)

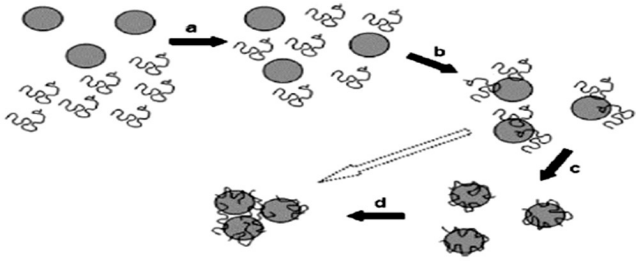

Fig.1 — Steps involved in the flocculation of particles by adsorbing polymer.

Adsorption of polymer chains particles occurs at a rate that depends primarily on the particle concentration. c) Adsorbed polymer chain on particle is attached by only a few segments of the chain. After a time, the polymer chain reaches its equilibrium adsorbed configuration with a characteristics distribution of loops, trains and tails. d) Flocculation occurs when particles have acquired enough adsorbed polymer to become destabilized, then collisions result in attachment, either by bridging, sweep-flocculation or for electrostatic reasons.

The efficacies of using these plant seeds: Cowpea seed (*Vigna unguiculata*), Fluted pumpkin seed (*Telfairia occidentalis*), Black Timber seed (*Brachystegia eurycoma*), Bambara nut seed (*Vigna subterranean*) and Horse radish seed (*Moringa oleifera*), as plant-based cationic coagulants are studied. The use of plant-based precursors was established because animal-based precursors are more expensive and difficult to source[6]. Crude extracts from the seeds are soluble cationic protein and have showed the ability to act as a natural polymer coagulant[7-12]. Thecoagulants studied have not been used in the decolourization of Azocarmine G dye.

In the present study, the potentials and performances of natural coagulants were studied for colour removal from Azocarmine G dye or acid red 101 (AR 101). The effects of *p*H, coagulant dosage, dye concentration, settling time and temperature on the coagulation-flocculation process were investigated and the optimal conditions were obtained. Polymer adsorption studies were done extensively following adsorption capacity, adsorption isotherms and adsorption kinetics.

Experimental Section

Preparation of natural coagulants seed powder

Sample 1: *Vigna unguiculata*
Sample 2: *Telfairia occidentalis*
Sample 3: *Brachystegia eurycoma*
Sample 4: *Vigna subterranean*
Sample 5: *Moringa oleifera*

Coagulant precursors were prepared as follows:

Dried seeds of *Vigna unguiculata* were purchased from local market of Enugu city. Matured seeds showing no signs of discolouration were used.

Matured pods containing *Telfairia occidentalis* seeds were purchased from local market of Enugu city. The seeds were removed from the pod, dried under sun for days, and the external shells were removed. Matured seeds showing no signs of discolouration, softening or extreme desiccation were selected.

Wet seeds of *Brachystegia eurycoma* were purchased from local market of Enugu city. Matured seeds showing no signs of discolouration were used. The seeds were de-hulled and sun dried.

Powder of *Vigna subterranean* was bought from local market of Enugu city.

Moringa oleifera seed pods were purchased from local market of Enugu city. Matured seeds showing no signs of discolouration, softening or extreme desiccation were used. The seeds were de-hulled and sun dried.

The dry seeds of the five samples were grounded to fine powder (63 – 600 μm) using an ordinary food processor (Model BL 1012, Khind) to achieve solubilisation of active ingredients. The seed powders were then ready for extraction of the active components.

Extraction of active component

The active component from coagulants was extracted by adding 2 g of powdered samples to 100 mL distilled water. Magnetic stirrer (Model 78HW-1, U-Clear England) stirred the stock solution vigorously for 20 min at room temperature to promote water extraction of the coagulant proteins. Filter paper (What. no. 42, 125 mm diameter) filtered the suspension. The filtrate portions were used as coagulant at required dosages. Fresh solutions were prepared daily and kept refrigerated to prevent any ageing effects (such as change in *p*H, viscosity and coagulation activity). Before each experiment, solutions were shaken vigorously and used immediately for each sequence of experiment.

Characterization of the coagulants

Yield, bulk density, moisture content, ash content, protein content, fat content and fibre content of the seed powders were determined by the standard official methods of analysis[13], while carbohydrate content was calculated by difference. Surface structures and morphologies of the seed powders were studied using scanning electron microscope (SEM, Phenom Prox., world Eindhoven, Netherlands).

Buffered solution

All assays were done in a *p*H-stable medium. Buffered solutions for the coagulation studies (Table 1) were prepared by the standards established according to the National bureau of standards (NBS, US) and standardized using a digital HANNA *p*H meter. All reagents used for *p*H analysis were of analytical purity grade.

Spectrophotometric decolourization procedures

Preparation of dye simulated wastewater and absorption spectrum determination

Acid red 101 (AR 101), water soluble dyewas provided by May & baker England with a molecular structure as shown in Fig. 2. The dye characteristics are summarized (Table 2). Dye with Commercial purity was used without further purification. The absorption spectrum of the dye was obtained by dissolving 1000 mg/L of AR 101 in distilled water. A sample of the solution was scanned against the blank of distilled water in the range of 250 – 850 nm using UV-V is spectrophotometer (Shimadzu, Model UV-1800). Stock solution of 1000 mg/L of dye was prepared by dissolving accurately weighed amounts of AR 101 in separate doses of 1L distilled water. The desirable experimental concentrations of 20-120 mg/L were prepared by diluting the stock solution with distilled water when necessary. The wavelength of maximum absorbance (λ_{max}) and calibration curve at λ_{max} were determined.

Coagulation studies

A conventional jar test apparatus (Phipps and Bird, VA, USA) equipped with six beakers of 1L capacity and six paddle stirrers was used to perform the coagulation-flocculation experiment. The jar test was conducted to evaluate the performances of the active agent extracted based on standard methods[11, 14, 15]. The procedure involved 4 min of rapid mixing at 100 rpm. The mixing speed was reduced to 40 rpm for another 25 min. The additional centrifuging (5000 rpm for 5 min) was performed to obtain clear liquid for all samples before analysis. All the suspensions were left for settling (60-540 min). Supernatant samples were withdrawn (after settling) for absorbance analysis using UV-V is spectrophotometer at set maximum wavelength of 516 nm. Colour removal was analyzed as a decrease in optical density measurement at 516 nm. The coagulation experiments were carried out at different operating conditions (Table 3). Removal efficiency was obtained according to Eq. 1:

$$\text{Colour removal (\%)} = \left(\frac{C_0 - C}{C_0}\right) \times 100 \quad \ldots (1)$$

where, C_0 and C are the initial and final colour

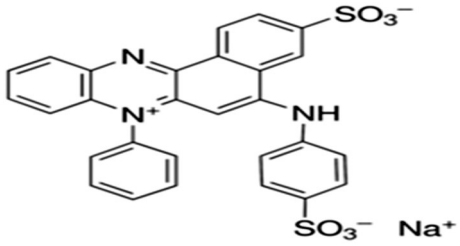

Fig. 2 — Structure of Azocarmine G (AR 101).

Table 2 — Physical properties of Azocarmine G.

Property	Data
Chemical name	Azocarmine G
Chemical formula	$C_{28}H_{18}N_3NaO_6S_2$
C.I number	50085
C.I name	Acid Red 101.
Class	Quinone - imine
Molecular Weight	579.58
CAS number	25641-18-3
UV/Visible Absorbance	Max. (Water): 510 + 6nm.

Table 1 — Buffer solutions

Buffers	Preparations
2.00	25 mL of 0.2M Potassium chloride was mixed with 6.5 mL of 0.2M Hydrochloric acid, diluted and made up to 100 mL using distilled water.
4.00	50 mL of 0.1M Potassium hydrogen phthalate was mixed with 3.0 mL of 0.1M Sodium hydroxide diluted and made up to 100 mL using distilled water.
6.00	50 mL of 0.1M Potassium hydrogen phosphate was mixed with 5.6 mL of 0.1M Sodium hydroxide diluted and made up to 100 mL using distilled water.
8.00	50 mL of 0.1M with respect to both Potassium chloride and Boric acid was added to 3.8 ml of 0.1M Sodium hydroxide, diluted and made up to 100 mL using distilled water.
10.00	50 mL of 0.1M with respect to both Potassium chloride and Boric acid was added to 43.7 mL of 0.1M Sodium hydroxide, diluted and made up to 100 mL using distilled water.
12.00	25 mL of 0.2M Potassium chloride was mixed with 6.0 ml of 0.2M of Sodium hydroxide, diluted and made up to 100 mL using distilled water.

Table 3 — Experimental operational parameter details for decolourization process.

Operational parameters	*p*H	Coagulant dosages (mg/L)	Dye concentration (mg/L)	Settling time (min)	Temperature (K)
Effect of *p*H	2, 4, 6. 8, 10 and 12	600	120	420	303
Effect of Coagulant dosage	2	200, 400, 600, 800 and 1000	120	420	303
Effect of Initial dye concentration (IDC)	2	200	20, 40, 60, 80, 100 and 120	420	303
Effect of Settling time	2	200	120	60, 120, 180, 240, 300, 360, 420, 480 and 540.	303
Effect of Temperature	2	200	120	420	303, 313, 323, 333, 343, 353

concentrations (mg/L) in dye solutions before and after coagulation-flocculation treatment, respectively.

Decolourization determination

Colour measurement was determined adopting standard dilution multiple method[16] and by comparing absorbance/concentration from a calibration curve. Decolourization of AR 101 dye was determined by monitoring the decrease in the absorbance peak at the maximum wavelength of 516 nm. Dye concentration of the supernatant (from coagulation experiment) was measured using UV-Vis spectrophotometer (Shimadzu, model 1800). The study was conducted by varying few experimental parameters including *p*H, coagulants dosages, initial dye concentrations (IDC), time and temperature. The *p*H was adjusted to the desired value using 0.1M HCL and 0.1M NaOH.

Polymer adsorption studies

The adsorption mechanism studied shows the ability of organic polymer coagulants adsorbing wastewater particles. Polymer adsorption chains mostly occur due to some attraction between polymer segments and particle surfaces. A widely accepted model of an adsorbed polymer chain[17], is shown in Fig. 3. In the model, particles are attached to the polymers surfaces in trains, polymers are projected into the solutions in tails, following the formation ofloops in trains. The extent of adsorption and formation of tails and loops depends greatly on the interaction of polymer segments with particle surfaces.

Polymer adsorption capacity

The parameter widely used in adsorption processes to show the extent of adsorption is the adsorption capacity (q). Contaminant removal by coagulation-flocculation mostly occurs in two stages for all the mechanisms applied. For example, in charge

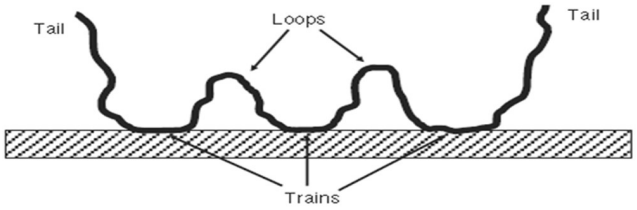

Fig. 3 — Formation of adsorbed polymer chain

neutralization mechanism, there is destabilization of colloids which may be governed by chemical interactions between molecules of the coagulants (cationic, positively charged) and of the contaminant (anionic, negatively charged). Then, once the coagulants-contaminant complex is formed, flocs begin to grow by adsorption mechanisms. Previous studies found coagulation capacity (q) a suitable adsorption evaluation parameter[4]. Polymer adsorption capacity (q_t) at any time was determined according to the following equation (2):

$$q_t\ (mg/g) = \frac{(C_o - C_t)\,V}{M} \quad \ldots (2)$$

where, C_o is the initial contaminant concentration (mg/L), C_t is the contaminant concentration at time t in the bulk solution (mg/L), V is the volume of solution (L), and M is the coagulants mass (mg/L).

Polymer adsorption isotherm theory

An isotherm shows the relationship of the distribution of adsorbate between the adsorbed phase and the solution phase equilibrium. The capacity of the polymers is described by its equilibrium adsorption isotherm. The purpose of the adsorption isotherms is to relate the particles concentration in the bulk solution and the amount of particles adsorbed at the interface[18]. Three isotherm models were analyzed in the present work: Langmuir, Freundlich, and Temkin models.

Langmuir model is based on the assumption that each site is capable of adsorbing one molecule, resulting in a monolayer-one molecule thick over the entire surface[19]. The linear form of Langmuir isotherm equation is given as:

$$\frac{C_e}{q_e} = \frac{1}{q_{max} K_L} + \frac{1}{q_{max}} C_e \quad ...(3)$$

where, q_{max} is the maximum capacity (mg of contaminant/g of coagulants) for complete monolayer adsorption and K_L (L/mg) is Langmuir adsorption constant. The essential characteristics of Langmuir equation can be expressed in terms of dimensionless separation factor, R_L, defined as [20]:

$$R_L = \frac{1}{1+K_L C_o} \quad ...(4)$$

R_L value implies the adsorption to be unfavourable ($R_L>1$), linear ($R_L=1$) favourable ($0<R_L<1$), or irreversible ($R_L= 0$).

Freundlich model is based on sorption onto a heterogeneous surface of varied affinities[21]. The linear form of Freundlich isotherm is given as:

$$\ln q_e = \frac{1}{n} \ln C_e + \ln K_F \quad ...(5)$$

where K_F (mg/g (l/mg)$^{1/n}$) is a Freundlich constant that indicates the sorption capacity of the polymer. n is a Freundlich adsorption order (dimensionless) that represents the parameter characterizing quasi-Gaussian energetic heterogeneity of the adsorption surface[22].

Temkin model was derived from Langmuir adsorption isotherm by inserting the condition that the heat of adsorption decreases linearly with surface coverage[23]. Temkin model is expressed in Eq. 6 as:

$$q_e = \left(\frac{RT}{b_T}\right) \ln (AC_e) \quad ...(6)$$

where RT/b_T = B (J/mol), which is the Temkin constant related to the heat of sorption, whereas A (l/g) is the equilibrium binding constant corresponding to the maximum binding energy. R (8.314J/mol k) is the universal gas constant and T (K) is the absolute solution temperature.

Polymer adsorption kinetics theory

Adsorption kinetic provides an invaluable insight into the controlling mechanism of adsorption processes which in turn governs mass transfer and the residence time[24]. The kinetic data were analyzed using pseudo-first order, pseudo-second order, Elovich and intra-particle diffusion model.

Lagergren proposed pseudo-first order kinetic equation[25], in the form of:

$$\text{Log } (q_e - q_t) = \log q_e - \frac{K_{f1}}{2.303t} \quad ... (10)$$

whereq_t is the amount of adsorbate adsorbed at time t (mg/g), q_e the adsorption capacity at equilibrium (mg/g), k_{f1} the pseudo-first order rate constant (min^{-1}), and t is the time (min). The value of the rate constant, k_{f1}, was determined from the plot of log (q_e - q_t) against t.

Pseudo-second order equation[26] predicts the behaviour over the whole range of adsorption with chemisorption being the rate controlling step and it is represented by:

$$\frac{t}{q_t} = \frac{1}{k_2 q_e} + \frac{1}{qe}\, t \quad ...(11)$$

where, k_2 is the pseudo-second order rate constant ($gmg^{-1}min^{-1}$). The linear plot of $\frac{t}{q_t}$ versus t gives $\frac{1}{qe}$ as the slope and $\frac{1}{k_2 q_e}$ as the intercept. The initial adsorption rate h (mg^{-1} min^{-1}) at t = 0 is defined as follows[27]:

$$h = k_2 q_e^2 \quad ...(12)$$

q_e is obtained from the slope of $\frac{t}{q_t}$ versus t and k_2 from the intercept. h is obtained from the Eq. (12).

Elovich[28] kinetic model equation, one of the most useful methods describing chemisorption processes, is defined as;

$$q_t = \frac{1}{\beta} \ln(\alpha\beta) + \frac{1}{\beta} \ln t \quad ...(13)$$

where α ($mgg^{-1}min^{-1}$) is the initial sorption rate and β (gmg^{-1}) is related to the extent of surface coverage and activation energy for chemisorption. The value of $(\frac{1}{\beta})$ is indicative of the available number of sites for adsorption while $\frac{1}{\beta}\ln(\alpha\beta)$ is the adsorption quantity when ln t = 0.

Intra-particle diffusion model[29] is calculated in order to gain insight into the mechanisms and rate controlling steps affecting the kinetics of adsorption. The model is expressed as:

$$q_t = k_3 t^{½} + C \quad ...(14)$$

where k_3 is the intra-particle diffusion rate constant ($mgg^{-1}min^{-1/2}$) and C is the intercept. k_3 and C can be evaluated from the intercept and slope of the plot of q_t versus $t^{½}$. The value of C relates to the thickness of the boundary layer. The large C implies the greater effect of the boundary layer[30].

Kinetic model validation

The suitability of the kinetic model to describe the adsorption process is validated by the normalized standard deviation, Δq (%) given by Eq. (15):

$$\Delta q\ (\%) = 100 \sqrt{\frac{\sum[(q_{exp} - q_{cal})/q_{exp}]^2}{df}} \quad ...(15)$$

where, d_f is the degrees of freedom of the fitting equation. The number of degree of freedom as follows N-n_p, where N is the number of data points and n_p is the number of parameters. q_{exp} (mg/g) and q_{cal} (mg/g) are the experimental and calculated adsorption capacities, respectively.

Results and Discussion

Characterization results

Proximate analysis

The proximate analyses of coagulant precursors were summarized in Table 4. The moisture content values show water absorption ability of the coagulants. High crude protein contents recorded in all the precursors especially in *Telfairia occidentalis* indicates the presence of protein, which is in agreement with the literatures that the protein contents of the precursors are cationic poly-peptides[7-11]. Fibre contents present established that the precursors were organic polymer with repeating small molecules that could extend as tails and loops when dispersed in water[5]. The proximate results justify the use of these seed powders as potential source of coagulant in this work.

SEM result

The SEM technique is used to analyze the surface morphological make-up of the polymeric coagulants (Fig. 4). SEM images show pores of different shapes and sizes for each coagulant. Rough surfaces of the coagulants were also observed. Particles could be adsorbed or attach it selves on these polymer chains forming bridging or electrostatic contacts. The pores and rough surfaces of the coagulants confirm adsorption as an important mechanism in coagulation-flocculation process. The morphologies of the coagulants also possess the compact-net structures. The compact-net structure is more favourable to contaminants flocculation due to bridge aggregation formation among flocs.

Absorption spectra of dye and calibration curve analysis

Figure 5 records the absorption spectra of 1000 mg/L stock solution of AR 101 in the wavelength range of 250-800 nm. The maximum wavelength (λ_{max}) obtained at visible UV range was 516 nm. The calibration curve test at different initial dye concentrations (10-120 mg/L)indicates Beer-Lambert's law was obeyed in the desired concentration range following the straight line graphs (Fig. 6) obtained from the plots[31]. The use of spectrophotometric method establishes an accurate method for determining the colour concentrations in aqueous solution following the result of the calibration analysis.

Effects of process parameters in decolourization procedure

Effect of pH

*p*H is an important factor to be considered in coagulation-flocculation process and must be controlled in order to establish optimum conditions in the process. The effectiveness of the coagulants in colour from dye is highly dependent on *p*H as shown in Fig. 7. The polymers showed high colour removals at low *p*H values.The highest removal efficiency was observed in TOC with 89.25% removal. Charge on the

Table 4 — Proximate compositions determination of the coagulant precursor

S/No.	Parameters	Values				
		Vigna unguiculata (Cowpea)	*Telfaria occidentalis* (fluted pumpkin seed)	*Brachystegia eurycoma* (Black timber)	*Vigna subterranean* (Bambara nut)	*Moringa oleifera seed*
1.	Yield	11.5	38.40	28.31	14.6	32.68
2	Bulk density (g/mL)	0.299	0.354	0.235	0.241	0.425
3.	Moisture Content (%)	9.0	12.58	7.25	10.0	5.02
4.	Ash content (%)	3.48	1.52	3.48	2.97	2.12
5.	Protein content (%)	25.14	55.09	19.77	18.15	39.34
6.	Fat content (%)	0.53	17.17	10.53	6.30	19.47
7.	Fibre content (%)	6.78	0.87	2.20	1.64	1.16
8.	Carbohydrate (%)	55.07	12.77	56.76	60.94	32.89

hydrolysis products of dye particles and precipitation of polymeric hydroxides are both controlled by *p*H variations[32]. The functional group of the acid dyeis anionic, hydrolyses products of the organic biopolymers can neutralize the negative charges on dye molecules followed by flocculation mainly by polymer adsorption and charge neutralization mechanisms. These mechanisms played a predominant role in the coagulation-flocculation process due to optimum *p*H values. Generally, adsorption of the natural organic contaminants (NOC) or NOC-polymer contaminant complexes onto polymer hydroxide precipitate forming at high *p*H is also limited[1]. As *p*H increases, natural organic compounds become more negatively charged and polymer hydrolysis species become less positively charged, resulting in less adsorption tendency. For these reasons, coagulation-flocculation of NOC in wastewatersis more efficient at low *p*H conditions.The polymer products react with anionic functional groupsof NOC to precipitate as a polymer-NOC. Similar results were reported by[1, 4, 33].

Effect of coagulant dosages

The result shown in Fig. 8 indicates that the removal efficiencies decrease with increasing dosages, except in TOC and MOC that were the reverse. The highest

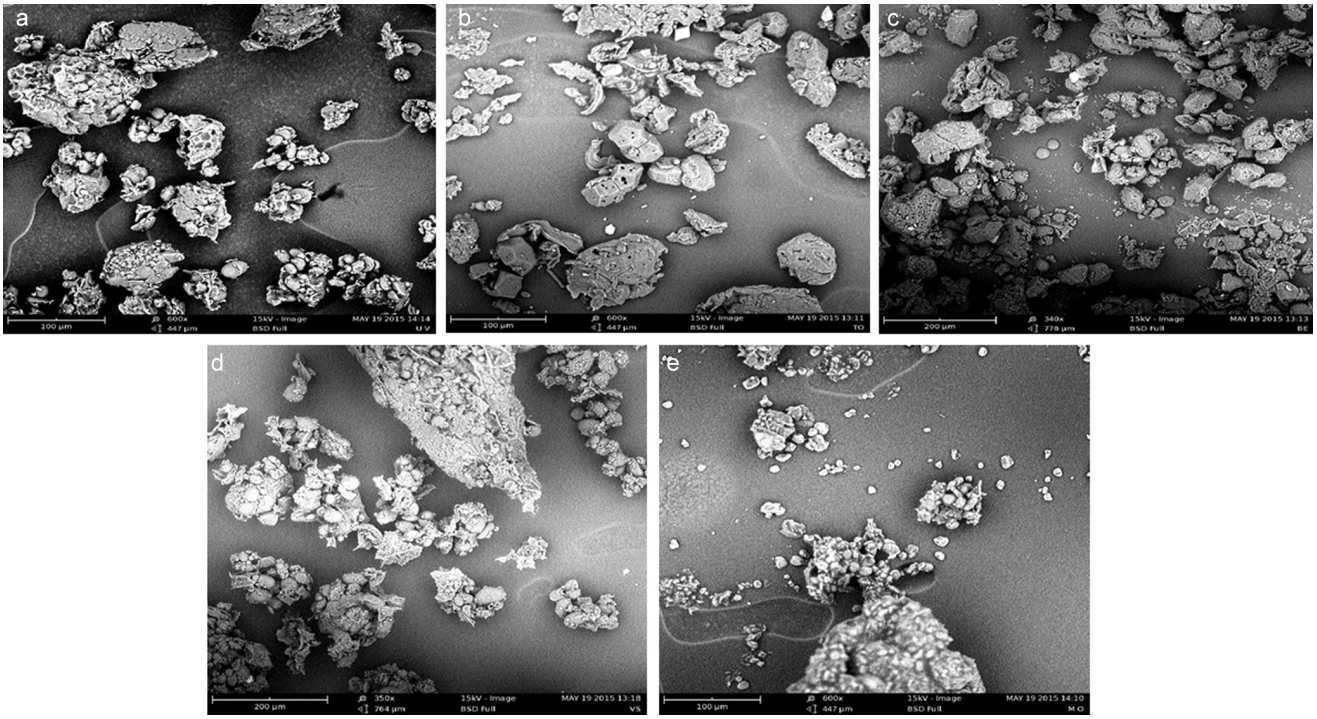

Fig. 4 — SEM micrographs of: (a) *Vigna unguiculata* coagulant (VUC); (b) *Telfairia occidentalis* coagulant (TOC); (c) *Brachystegia eurycoma* coagulant (BEC); (d) *Vigna subterranean* coagulant (VSC); (e) *Moringa oleifera* coagulant (MOC).

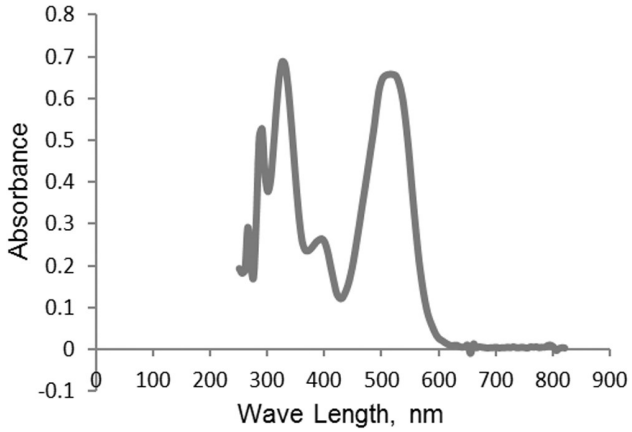

Fig . 5 — Spectrum peak plot for AR 101

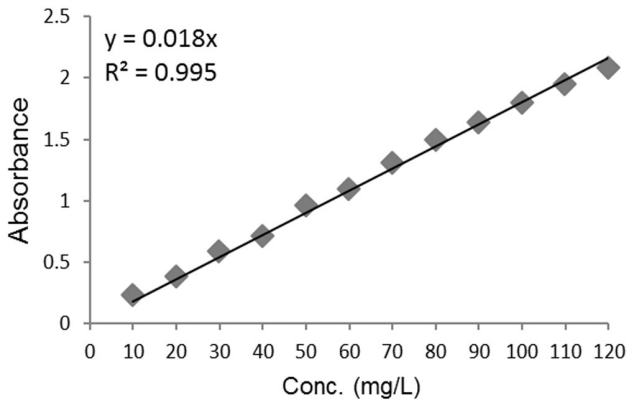

Fig. 6 — Calibration curve for AR 101 at a wave length of 516 nm.

removal efficiency of 91.21% wasachieved at 800 mg/L dosage for TOC. The high removal efficiencies of >50% found in all the coagulants for 200 mg/L dosage confirms that charge-neutralization and adsorption mechanism to be predominant mechanism in the process. Positive charge species are responsible for removal of particles by charge neutralization. The use of cationic polymer for coagulation-flocculation of negatively-charged colour particles is needed, because strong adsorption affinity and neutralization of the particle charges could occur. Increase in the coagulant dosages (1000 mg/L TOC and 1000 mg/L) resulted in a decrease in the removal efficiency as observed in Fig. 8, which implies that overdosing has occurred. Overdosing degrades supernatant quality and makes particles not to coagulate well. Also with excess polymer, the particle charges may be reversed. Increase in dosage that resulted in high efficiency as observed in TOC and MOC confirms that sweep-flocculation and adsorption mechanism was predominant in the removal process. The high efficiency at high dosageobserved in both coagulants could also give rise to chain bridging and adsorption mechanism due to polymer nature as explained in Fig. 1[1].

Effect of initial dye concentration (IDC)

The concentrations of dye provide an important driving force to overcome all the mass transfer resistance between the aqueous and solid phases[34]. As observed in Fig. 9, increase in IDC gave an increase in colour removal efficiencies for all the coagulants. This may be explained by the fact that a lower concentration gradient caused a slower transport due to a decreased diffusion coefficient or decreased mass transfer coefficient[35]. Dye concentrations also play an important role in the coagulation-flocculation process because it determines the extent of particle transfer. As the influent concentration increased, dye loading rate increased and the driving force increased for mass transfer. Highest efficiency was observed at 120 mg/L for TOC with removal efficiency of 91.50%.

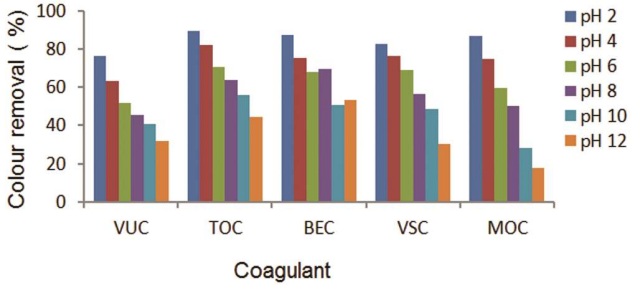

Fig. 7 — Effect of *p*H on the colour removal (%) using polymer coagulants. IDC = 120 mg/L, coagulant dosage = 600 mg/L, settling time = 420 min, temperature = 303 K.

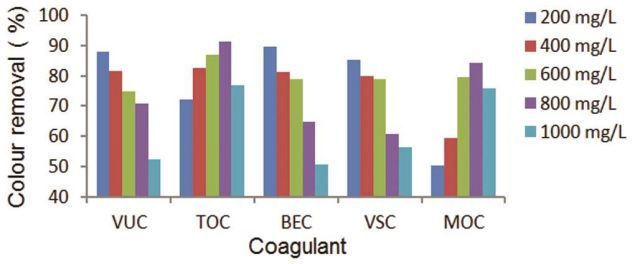

Fig. 8 — Effect of coagulant dosage on the colour removal (%) using polymer coagulants. IDC =120 mg/L, *p*H = 2, settling time = 420 min, temperature = 303 K.

Effect of temperature on the colour removal efficiency

Colour removal efficiency decreases as solution temperature increases (Fig. 10). The optimum solution temperature was 303 K. This could be as a result of high solution temperature breaking polymer chains, reducing the surface adsorption sites of the coagulants. Also, high temperature reduces the flocs growth which in turn reduces coagulation-flocculation process.

Effect of settling time on the percentage colour removal

The effect of coagulant performances was analyzed at different settling time. Flocs formation involves

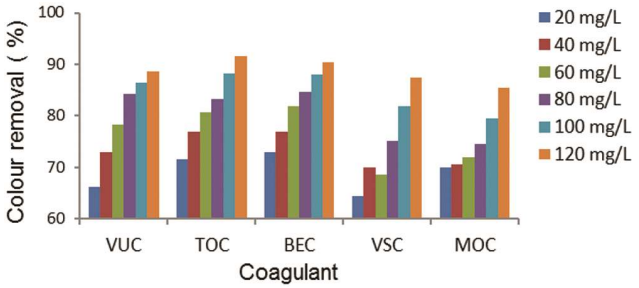

Fig. 9 — Effect of IDC on the colour removal (%) using polymer coagulants at their optimum dosages. *p*H = 2, settling time = 420 min, temperature = 303 K.

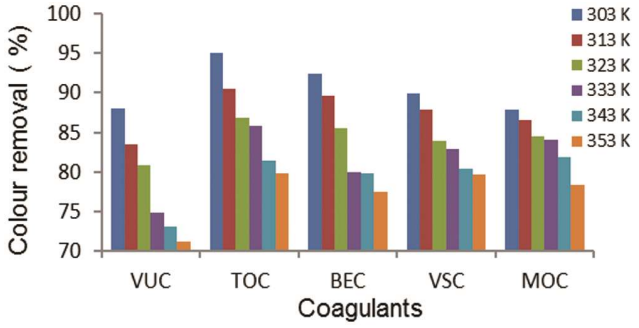

Fig. 10 — Effect of temperature on the colour removal (%) using polymer coagulants at their optimum dosages. *p*H = 2, IDC = 120 mg/L, temperature = 303 K

both interactions of coagulant hydroxide precipitate following hydrolyses reaction and contact with particles. In Fig. 11, the highest reduction in concentration was observed in 800 mgTOC/L followed by 200 mgBEC/L resulting in removal efficiencies of 93.4% and 91.4%, respectively. This rapid reduction indicates a rapid coagulation-flocculation process, which was fast at onset resulting to over 76% removal at first 120 min. The longer process time is also a confirmation of presence of polymer adsorption mechanism, showing that sorption processes takes longer time to complete[35]. The concentrations did not vary significantly after 420 min showing that equilibrium can be assumed to have been achieved after 420 min and destabilization of the aggregate flocs could set in after this time. This could be due to saturation of the active sites which does not allow further polymer adsorption and also prolonged settling time.

Polymer adsorption results

Polymer adsorption capacity for colour removal from dye wastewater

The effect of settling time on the polymer adsorption capacity for colour at different coagulants and optimum doses is shown in Fig. 12. This figure shows that the adsorption capacity for colour increases with increase in settling time. The plot of sorption capacity clearly shows that there was a rapid

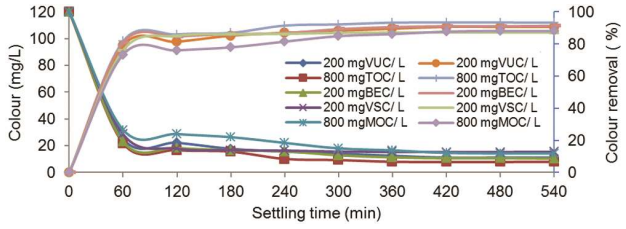

Fig. 11 — Effect of settling time on the colour removal (%) using polymer coagulants at their optimum dosages. *p*H = 2, IDC 120 mg/L, temperature = 303 K.

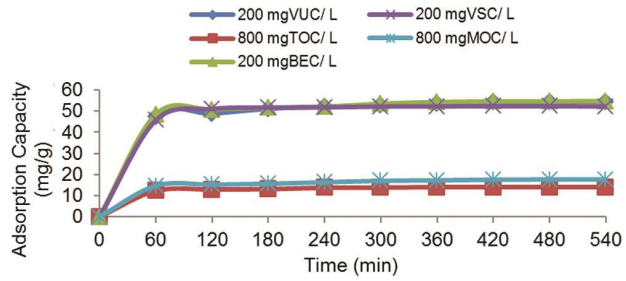

Fig. 12 — Effect of coagulant dosages and settling time on coagulation-adsorption capacity. *p*H = 2, IDC = 120 mg/L, temperature = 303 K

increase in adsorption capacity during the first 60 min. The fast adsorption at the initial stage may be due to the higher driving force (contaminants concentration) making fast transfer of particles from the bulk of contaminant region to the polymer surface. Also, due to high avalability of the uncovered surface area and remaining active sites of the coagulants.

Polymer adsorption isotherm

Figures 13-16 shows the Langmuir, Freundlich and Temkin isotherm plots. Table 5 summarizes all the isotherm parameters and correlation coefficient (R^2) values obtained from the isotherm models applied for the polymer adsorption of colour on the coagulants. From the table, the Langmuir model yielded highest

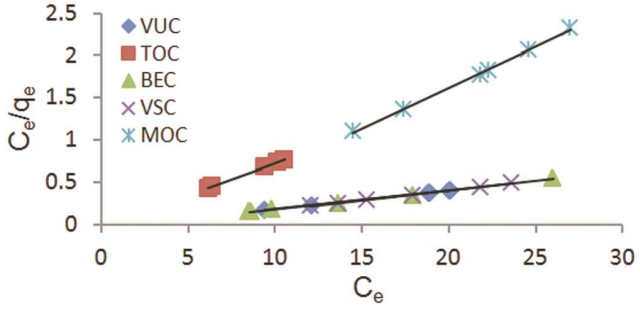

Fig. 13 — Langmuir isotherm for colour removal from AR 101 dye at 303K.

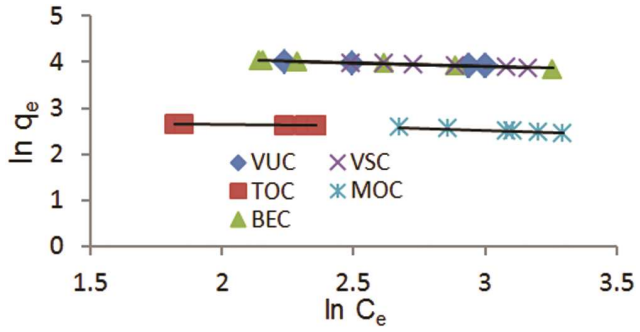

Fig. 14 — Freundlich isotherm for colour removal from AR 101 dye at 303K.

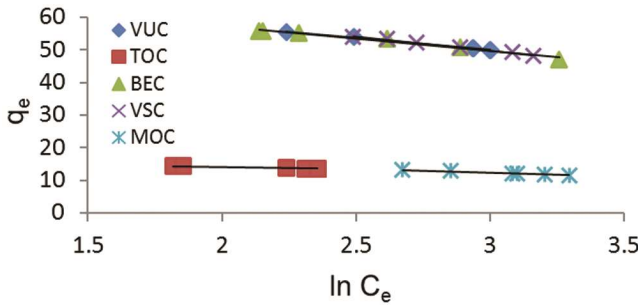

Fig. 15 — Temkin isotherm for colour removal from AR 101 dye at 303K.

values of the correlation coefficient R^2 (>0.991) compared to Freundlich models, indicating a monolayer adsorption mechanism. Isotherm studies show that adsorption of contaminant particles on the polymer surfaces occurred more according to the mechanism of chemisorption which involves sharing of electrons between the adsorbate molecules and the surface of polymer resulting in a chemical reaction. The value of R_L obtained gave a favourable colour adsorption onto polymer surfaces.

Polymer adsorption kinetics results

Pseudo-first order kinetics, pseudo-second order kinetics, Elovich kinetics and Intra-particle diffusion plots for colour removal were shown in Figs. 17-20. The kinetic constant for the four kinetic models are summarized in Table 6. The correlation coefficients for the models were relatively low as compared with those for the pseudo-second order model and also the experimental data shows a good agreement with the pseudo second-order kinetic model data, with the lowest normalized standard deviation, Δq (%) values ranging between 0.96% and 3.15%. The fitting of pseudo-second order kinetic model with high coefficient of determination (R^2>0.993) further validates coagulation-flocculation process as a second-order process. Elovich model agreement also gave a further insight to the adsorption-chemisorption process. This suggested that the overall rate of the adsorption process was controlled

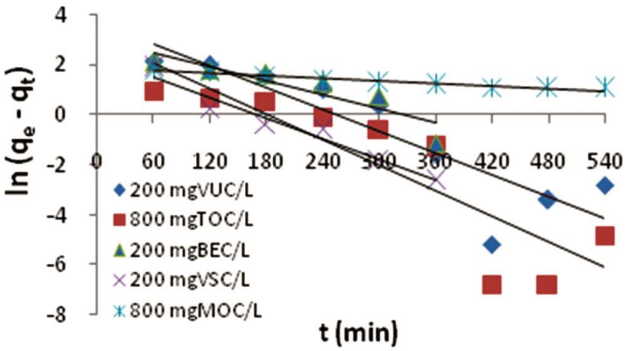

Fig. 16 — Pseudo - first order kinetics for the colour removal at different coagulants at their optimum dosages.

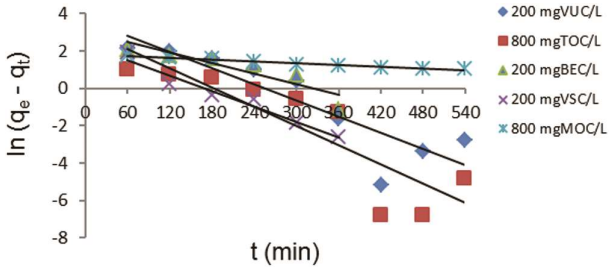

Fig. 17 — Pseudo - first order kinetics for the colour removal at different coagulants at their optimum dosages.

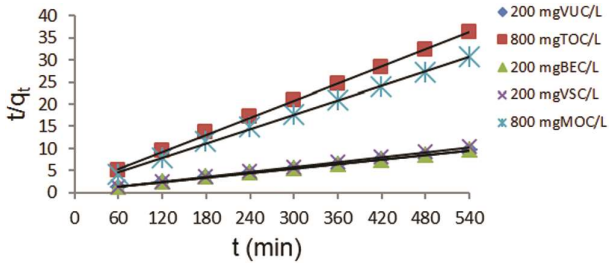

Fig. 18 —Pseudo - second order kinetics for the colour removal at different coagulants at their optimum dosages.

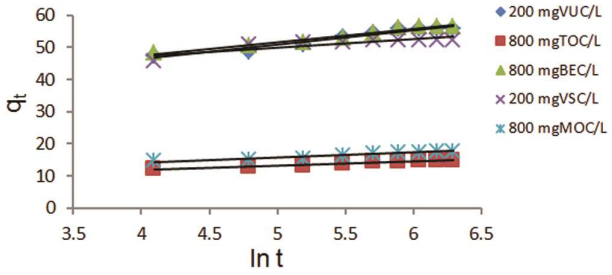

Fig. 19 — Elovich kinetic model for the colour removal at different coagulant at their optimum dosages

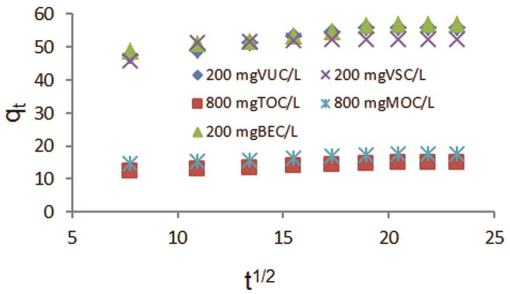

Fig. 20 — Intraparticle diffusion model for the the colour removal at different coagulants at their optimum dosages.

Table 5 — Langmuir, Freundlich and Temkin isotherm parameters for adsorption mechanism study

	Langmuir				Freundlich			Temkin		
Polymers	q_{max} (mg L/mg)	K_L (L/mg)	R_L^2	R_L	K_f (mg/g(L/mg)$^{1/n}$)	n	R_F^2	A (L/mg)	B	R_T^2
VUC	12.99	1.83	1	0.0046	75.26	-7.35	0.993	4.5E-05	-7.15	0.994
TOC	47.62	0.58	0.999	0.014	16.25	-13.9	0.998	1.4E-05	-1.02	0.998
BEC	45.45	0.49	0.997	0.017	76.71	-6.85	0.968	6.9E-04	-7.54	0.976
VSC	43.48	0.40	0.999	0.020	82.68	-5.92	0.989	1.6E-04	-8.64	0.992
MOC	10.31	0.29	0.998	0.028	22.65	-5.00	0.988	3.4E-04	-2.49	0.992

Table 6 — Adsorption kinetics model parameters

		Pseudo-first order kinetics					Pseudo-second order kinetics					Elovich kinetics		
Dye	Coagulants dosages (mg)	q_e, exp (mg/g)	q_e, cal (mg/g)	K_{F1} (min^1)	R^2	Δq (%)	q_e, cal (mg/g)	K_2 (g/mg min)	R^2	h (mg/g min)	Δq (%)	a	b	R^2
AR 101	200 mgVUC/L	55.95	39.41	0.014	0.788	10.45	58.82	0.0501	0.999	173.34	1.814	2.57E+03	0.223	0.957
	800 mgTOC/L	14.89	22.22	0.017	0.763	17.4	15.625	0.0408	0.999	9.96	1.745	1.79E+02	0.744	0.963
	200 mgBEC/L	56.65	20.55	0.009	0.801	22.53	58.824	0.0517	0.999	178.90	1.357	7.79E+03	0.242	0.959
	200 mgVSC/L	52.35	10.55	0.013	0.957	28.23	55.556	0.1565	0.999	483.03	2.165	6.01E+06	0.394	0.926
	800 mgMOC/L	13.23	6.265	0.001	0.948	18.61	18.519	0.0399	0.999	13.68	5.423	2.96E+02	0.652	0.951

more by chemisorption which involved valence forces through electrons sharing between the polymer and contaminant. Intra-particle diffusion kinetic model is not the sole rate determining step because the linear plot did not pass through the origin[36].

Conclusion

Present study analyzed the feasibility of colour removal from acid red 101 using natural organic polymers as coagulants. The coagulants studied have been found to be highly effective in the decolourization process. The extractive method employed in obtaining the coagulant agents is a suitable and also helps insludge load reduction. Operational parameters studied (*p*H, coagulant dosage, dye concentration, settling time and temperature) extremely influence the colour removal process. Adsorption mechanism is very important in the coagulation-flocculation process using natural (plant-based) coagulants. Adsorption process occurred more as a second-order rate process, showing that the rate depends on the square of the particle concentration. Thus, at high particle concentrations, flocculation rates become very high.

References

1 Zhu G, Zheng H, Zhang Z, Tshukudua T, Zhang P & Xiang X, *Chem Eng* J, 178 (2011) 5.
2 Anouzla A, Abrouki Y, Souabi S, Safi M & Rhbal H, *J Hazard* Mater, 166 (2009) 1302.
3 Beltrán-Heredia J, Sánchez-Martín J, Delgado-Regalado A & Jurado-Bustos C, *J Hazard Mater*, 170 (2009) 43.
4 Beltran-Heredia J, Sanchez-Martin J & Davila-Acedo M A, *J Hazard* Mater, 186 (2011) 1704.
5 Bolto B & Gregory J,*Water Res*, 41 (2007) 2301.
6 Antov M G, Marina B & Petrovic N J, *Bioresour* Technol, 101 (2010) 2167.
7 Mariângela S S D & André O C, *Biol* Plant, 44 (2003) 417.
8 Kuku A, Etti U J &Ibironke I S, *Plant Physiol* Biochem, 39 (2014) 137.
9 Ikegwu O J, Oledinmma N U, N wobasi V N & Alaka I C, *J food Technol*, 7 (2009) 34.
10 Massawe F J, Mwale S S, Azan-Ali, S N & Roberts J A, *African J Biotechnol*, 4 (2005) 463.
11 Ndabigengesere A, Narasiah K S &Talbot B G, *Water* Res, 29 (1995) 703.
12 Obiora-Okafo I A,Menkiti M C & Onukwuli O D, *Int J Appl Sci* Math, 1 (2014) 15.
13 A O A C, *Official Methods of Analysis*, Association of Official Analytical Chemists, 15th ed,Washington D C, U S A, 1990.
14 Okuda T, Baes A U & Nishijima W, Okada M, *Water Res*, 33 (1999) 3373.
15 Abidin Z Z, Ismail N,Yunus R, Ahamad I S & Idris A, *Environ Technol*, 32 (2011) 971.
16 Obiora-Okafo I A & Onukwuli O D, *Int J Sci Eng* Res, 6 (2015) 693.
17 Napper D H, *Polymeric Stabilization of Colloidal Dispersions*, Academic Press London, (1983) 158.
18 Eastoe J & Dalton J S, *Adv J Colloid Interface Sci*, 85(2000) 103.
19 Langmuir I, *J Am Chem Soc*, 40 (1918) 1361.
20 Hall H R, Eagleton L C, Acrivos A &Vermeulen T, *I EC Fundam* J, 5 (1966) 212.
21 Freundlich H, *Colloid and capillary chemistry*, Mathuen London(1926) 110.
22 Roop G & Meenakshi G, *Activated carbon adsorption; adsorption Energetics, Models and isotherm Equations*, Taylor and Francis Group (2005) 120.
23 Temkin M J & Pyzhev V, *Acta Physiochem* URSS,12 (1940) 217.
24 Zhang T, Li Q R, Liu Y, Duan Y L & Zhang W Y, *Chem Eng J,* 168 (2011) 665.
25 Lagergren S & Svenska B K, *Kungsven Velenska-Psad Hand,* 24(1898) 6.
26 Ho Y S & Mc Kay G, *Process Biochem*, 34 (1999) 451.
27 Khated A, Nemr A E, El-Sikaily A &Abdelwahab O, *J Hazard Mater*, 165 (2008) 100.
28 Aharoni C & Tompkins F CIn: Eley D D, Pines H & Weisz P B (Eds), *Adv Catal, Related Subj 21*, Academic Press, New York(1970).
29 Weber W J & Morris J C, *J Saint Eng Div Proceed Am SOC, Civil Eng,* 89 (1963) 31.
30 Vimonses V, Lei S, Jin B, Chow C W K & Saint C, *Appl Clay Sci*,43 (2009) 465.
31 Jeffrey G H, Bassat J, Mendham J & Denney R C, *Textbook of quantitative chemical analysis*, 5th ed Longman Scientific &Technical, (2005) 649.
32 Li G & Gregory J, *Water Res*, 25 (1991) 1137.
33 Moghaddam S S, AlaviMoghaddam M R & Arami M, *J Hazard Mater*, 175 (2010) 651.
34 Hameed B H, Mahmoud D K & Ahmad A L, *J Hazard Mater*,158 (2008) 65.
35 Ouvrard S,Simonnot M O, De Donato P & Sardin M, *Ind Eng Chem Res*, 41 (2002)6194.
36 Ozacar M, Engil I A &Turkmenler H,*Chem Eng J,* 143 (2008) 32.